Structure and dynamics of hyaluronic acid semidilute solutions: A dielectric spectroscopy study

T. Vuletić,* S. Dolanski Babić,† T. Ivek, D. Grgičin, and S. Tomić
Institut za fiziku, Zagreb, Croatia

R. Podgornik
Department of Physics, Faculty of Mathematics and Physics and Institute of Biophysics, School of Medicine, University of Ljubljana, Ljubljana, Slovenia; J. Stefan Institute, Ljubljana, Slovenia; and Laboratory of Physical and Structural Biology, Eunice Kennedy Shriver National Institute of Child Health and Human Development, National Institutes of Health, Bethesda, Maryland, USA
(Received 13 November 2009; revised manuscript received 17 May 2010; published 23 July 2010)

Dielectric spectroscopy is used to investigate fundamental length scales describing the structure of hyaluronic acid sodium salt (Na-HA) semidilute aqueous solutions. In salt-free regime, the length scale of the relaxation mode detected in MHz range scales with HA concentration as $c_{\mathrm{HA}}^{-0.5}$ and corresponds to the de Gennes-Pfeuty-Dobrynin correlation length of polyelectrolytes in semidilute solution. The same scaling was observed for the case of long, genomic DNA. Conversely, the length scale of the mode detected in kilohertz range also varies with HA concentration as $c_{\mathrm{HA}}^{-0.5}$ which differs from the case of DNA ($c_{\mathrm{DNA}}^{-0.25}$). The observed behavior suggests that the relaxation in the kilohertz range reveals the de Gennes-Dobrynin renormalized Debye screening length, and not the average size of the chain, as the pertinent length scale. Similarly, with increasing added salt the electrostatic contribution to the HA persistence length is observed to scale as the Debye length, contrary to scaling pertinent to the Odijk-Skolnick-Fixman electrostatic persistence length observed in the case of DNA. We argue that the observed features of the kilohertz range relaxation are due to much weaker electrostatic interactions that lead to the absence of Manning condensation as well as a rather high flexibility of HA as compared to DNA.

DOI: 10.1103/PhysRevE.82.011922 PACS number(s): 87.15.H−, 77.22.Gm

I. INTRODUCTION

Dynamics of counterion atmosphere in the vicinity of polyelectrolytes can be used as an important structural tool in order to better understand their functional properties and is thus of fundamental importance also for various areas of bionanotechnology and biomedical sciences in general. In biological context, charged polyelectrolytes like deoxyribonucleic acid (DNA), ribonucleic acid (RNA), polypeptides and polysaccharides such as hyaluronic acid (HA) are essential for life and make their mark in many structural and functional aspects of the cellular environment [1]. DNA is in many respects a paradigm of a semiflexible highly charged polymer whose complex behavior was studied in great detail. In aqueous solutions it assumes a conformation of an extended statistical coil, whereas *in vivo* long genomic DNA is usually compactified to fit within the micron-sized nucleus of eukaryotic cells or even smaller nanoscale viral capsids [2].

HA is a member of the glycosaminoglycan family and is an alternating copolymer of D-glucuronic acid and N-acetyl glucosamine that occurs in connective tissue and mucous substances in the body. Similarly as in the case of DNA, HA always comes as a highly asymmetric salt with positive counterions, in our case as sodium salt Na-HA. In aqueous solutions its carboxyl groups are completely dissociated making HA a charged polyelectrolyte. In the crystalline form, HA covers a broad range of conformations depending on *p*H, whereas in solution HA is a single-stranded helix [3].

Parameters known to be relevant for the counterion dynamics in polyelectrolyte solutions include valency, strength of electrostatic interactions, concentration of polyions and added salt ions. Characteristic frequencies in collective counterion dynamics span several orders of magnitude ranging from kilohertz to megahertz. These characteristic frequencies were found to be directly correlated with the details of the counterion motion around polyions [4–8]. For the sake of completeness we reiterate that in the polyelectrolyte solutions one also finds a relaxation related to water, confined to the gigahertz range [4,9]. For the strongly charged polyelectrolytes such as DNA one distinguishes two distinct types of counterions: condensed counterions which are tightly bound to the polyions and free counterions. These counterion types are considered transient, meaning that there is a constant dynamic exchange between them. Relaxation mode arising from the collective motion of condensed counterions takes place in the kilohertz frequency range (low frequency, LF mode), whereas the mode associated with free counterion motion is detected in the higher megahertz frequency range (high frequency, HF mode). In the linear regime, i.e., for small applied ac electric fields, these relaxation modes probe directly the conformational features of either a single polyelectrolyte chain or the structure of an ensemble of many chains in solution. Our dielectric spectroscopy (DS) measurements on long DNA semidilute solutions [6,7] show that the measured fundamental length scale, probed by the LF mode, is equal to the size of the Gaussian chain composed of correlation blobs that scales as $c_{\mathrm{DNA}}^{-0.25}$ in the low added salt limit. In the high added salt limit the LF mode characteristic length scale goes over to the Odijk-Skolnick-Fixman (OSF) electrostatic persistence length L_{p} and scales as

*http://real-science.ifs.hr/; tvuletic@ifs.hr URL
†Present address: Department of physics and biophysics, Medical School, University of Zagreb, Croatia.

$L_p = L_0 + aI_s^{-1}$. Here L_0 is the DNA structural persistence length of 50 nm and I_s is the ionic strength of the added salt. On the other hand, the HF mode is probing the collective properties of the DNA solution which are characterized by the de Gennes-Pfeuty-Dobrynin (dGPD) correlation length or the solution mesh size, that scales as $c_{DNA}^{-0.5}$. This result was equally reported on diverse synthetic polyelectrolytes [4,5].

An intriguing issue is if and how the dielectric relaxation modes will change for polyelectrolytes, such as HA, which are much more flexible than DNA, i.e., how is the counterion dynamics affected when the structural persistence length becomes smaller than the dominating correlation length. We note that the double-stranded DNA (ds-DNA) is best described as a strongly charged semiflexible polyelectrolyte whose structural persistence length, L_0 close to 50 nm, is larger than the correlation length. Another interesting issue is what happens in the case of weakly charged polyelectrolytes, again such as HA, whose Manning charge density parameter $\eta < 1$, so that according to the Manning criterion no counterion condensation takes place. Here $\eta = zl_B/b$, where z is the valency of the counterion, b is the linear charge spacing and l_B is the Bjerrum length. The question then arises whether or not free counterions, in addition to their primary role, take over the role of condensed counterions as in strongly charged polyelectrolytes. In other words, do free counterions, in addition to oscillating between the correlated polyion chains in the solution, also perform an oscillatory motion along the polyion chain revealing in this way the conformational features of a single chain. Previous DNA studies have shown that the LF relaxation mode does not allow a clear-cut separation between condensed and free counterions as relaxation entities and that both of them contribute to various extent in different salt and DNA concentration regimes [7].

In this work we address these issues by characterizing the dynamic behavior of semidilute solutions of a sodium salt of hyaluronic acid (Na-HA). HA is a weakly charged polyelectrolyte whose disaccharide monomer is 1 nm long implying the Manning charge density parameter $\eta \approx 0.71$. The structural persistence length is about 9 nm [10] and is larger than the monomer size so that, according to the standard criterion, HA belongs to semiflexible polyelectrolytes, being much stiffer than the standard synthetic polyelectrolyte polystyrene sulfonate Na-PSS, but at the same time much more flexible than ds-DNA.

II. MATERIALS AND METHODS

In this study we used hyaluronic acid sodium salt from streptococcus equi sp. Fluka 53747 obtained from Sigma-Aldrich. The low protein content ≤ 1 is declared by the manufacturer. An average molecular weight is about 1.63×10^6 Daltons, implying 4000 monomers in average. For HA, disaccharide monomer is of molecular weight 401 g/mol and there is one Na^+ ion per HA monomer. This means that the molar concentrations of HA monomers, as well as Na^+ counterions are related by $c_{in}[\mathrm{mM}] = c_{HA}[\mathrm{mg/mL}] \times 2.5$ μmol/mg to the HA concentration by weight. We perform a systematic study of how the dielectric properties of these polydisperse long HA fragments in aqueous solutions evolve upon change of HA concentration and added salt over a range of two orders of magnitude. HA solutions were prepared as described previously (see Materials and Methods I in Ref. [7], preparation protocols I and II.1). A crude estimate of the crossover concentration between dilute and semidilute regime c^* based on the de Gennes arguments [11], and taking into account that the average HA fragments are 4 μm long, yields c^* of the order of 0.000 04 mg/mL, which is more than two orders of magnitude below the lower concentration bound in our experiments [12]. This means that we are effectively always in semidilute regime which has been studied in depth experimentally in the case of long polydisperse DNA fragments in aqueous solutions [7].

A. Capacitance chamber and the electrode polarization

Dielectric spectroscopy up to 100 MHz is usually performed with a capacitance chamber [13–17]. There, a sample solution is applied between the electrodes of a parallel plate capacitor and a frequency-dependent impedance is measured. We performed our measurements with an in-house designed chamber, with built-in temperature control. The chamber was connected in a four-terminal pair configuration to an Agilent 4294A precision impedance analyzer [15]. The measurement functions were conductance $G(\omega)$ and the capacitance in parallel $C_p(\omega)$, where $\omega = 2\pi\nu$ is frequency. These combine into complex admittance (inverse of complex impedance Z),

$$Y(\omega) = G(\omega) + \imath\omega C_p(\omega). \tag{1}$$

Admittance is sampled at 201 frequencies, i.e., at 33 points per frequency decade for the frequency range 100 Hz–110 MHz. A single frequency point is sampled with bandwidth BW=5 setting (longer acquisition time, but lower noise—BW=1 would be faster, however more noisy, and would demand averaging ten times for one point). In addition, three consecutive frequency sweeps are taken in order to average out the temperature variations. Total time for the spectrum measurement amounts to 120 s.

In the measurements with a capacitance chamber a well-known electrode polarization (EP) influences the results. EP is due to the rearrangement of ions and a buildup of spatial charge in the vicinity of the electrodes, which manifests itself as a large frequency-dependent capacitance, C_{EP}, in series with the sample chamber impedance—impedance of a capacitor containing a conducting dielectric. EP can be roughly represented in kilohertz range (for simple electrolytes at concentrations below 10 mM) by $C_{EP} = a \cdot \omega^{\alpha}$, where $\alpha \approx -2$. EP also strongly reduces measured conductance, G in the same low-frequency range. The effect is proportional to the ionic conductivity of the electrolyte, i.e., to its ionic strength I_s. The contributions (of polarization currents) due to the system of interest (e.g., polyelectrolyte, colloid) may be extracted only in the frequency range where they are of comparable or larger magnitude than EP effects. This practically limits dielectric spectroscopy below 100 MHz to studies of samples in electrolytes with I_s not above 10 mM [13–17].

Various experimental methods [4] aim to reduce the EP effect, e.g., four-contact measurement cells [18], electromag-

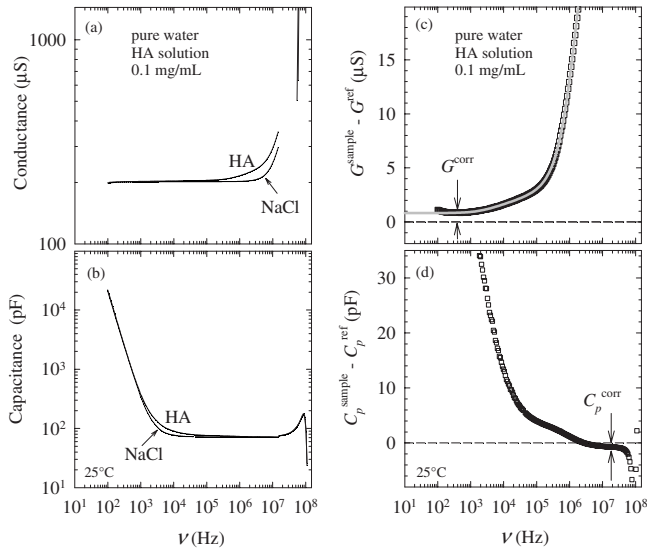

FIG. 1. (a),(b) Double logarithmic plot of the frequency dependence of the (a) conductance and capacitance for 0.1 mg/mL HA solution and the matching reference 0.14 mM NaCl solution. (c),(d) Frequency dependence of the *differential* admittance components $G(\omega)=G^{\text{sample}}(\omega)-G^{\text{ref}}(\omega)$ and $C_p(\omega)=C_p^{\text{sample}}(\omega)-C_p^{\text{ref}}(\omega)$. The correction constants are denoted G^{corr} and C_p^{corr}. The full line in panel (c) is the $G(\omega)$ spectrum calculated from the complex dielectric function fit (see text).

netic induction measurement methods or simple utilization of the microporous, platinum black electrodes (however, Pt-black deteriorates with repeated usage [16]). A different approach is to model the EP contribution to the sample impedance and consequently remove it. However, while this may be done in theory, in practice, every new polyelectrolyte solution presents itself as a system where the EP effect can have a different influence, and our incomplete understanding of this phenomenon reappears [17]. Even for a simple capacitance chamber there remain two experimental approaches for reduction of EP. The first one is to make measurements at different electrode separations [16]. Then, as EP effect is the only one dependent on the electrode surface area as opposed to the volume-dependent sample contribution, one can distinguish the two contributions. The second EP reduction approach is the reference subtraction method [4,19–21] which is used in our work. In addition to HA samples, the reference samples of a simple electrolyte NaCl were also measured and corresponding spectra subtracted from HA spectra in order to minimize stray impedances, including the free ion contribution and EP effects, and extract the response due to HA only [7]. Naturally, this method has limitations in the sense that the EP effects are not necessarily the same for the sample and reference solutions—an issue similar to the abovementioned EP modeling methods [4].

While recognizing its limitations, we have chosen the reference subtraction method, and designed our setup accordingly, as it allows for quick data analysis and high sample throughput (a sample is exchanged every 10 min) with a minimal sample volume (100 μL).

Figures 1(a) and 1(b) shows the 0.1 mg/mL HA pure water solution conductance and capacitance spectra in conjunction with data for 0.14 mM NaCl reference solution of matching conductance (matched at 100 kHz). The corresponding curves show only a small mismatch which indicates that the main contributions come from the free ion conduction or the EP effect, while the contribution of interest $G(\omega)$, $C_p(\omega)$, which is due to the polyion and its counterion atmosphere, is minor. Therefore, assuming that the conductivity contribution of each entity in the solution is additive [22], we have treated the contribution of interest additively,

$$G(\omega) = G^{\text{sample}}(\omega) - G^{\text{ref}}(\omega), \tag{2}$$

$$C_p(\omega) = C_p^{\text{sample}}(\omega) - C_p^{\text{ref}}(\omega), \tag{3}$$

and Figs. 1(c) and 1(d) shows the result of this subtraction. The contribution of the system of interest (i.e., the polyion and its counterion atmosphere) to conductivity $\sigma(\omega)=K[G(\omega)+\imath\omega C_p(\omega)]$ can be used to express its contribution to the complex dielectric function $\varepsilon(\omega)=\varepsilon'(\omega)-\imath\varepsilon''(\omega)=\sigma(\omega)/(\imath\omega\varepsilon_0)$ (here K is the geometrical sample chamber constant $K=l/S$, l is the electrode separation and S the surface area, and ε_0 is the permittivity of vacuum). We arrive to the final expression for the imaginary and real part of dielectric function:

$$\varepsilon''(\omega) = \frac{K(G^{\text{sample}}(\omega) - G^{\text{ref}}(\omega) - G^{\text{corr}})}{\omega\varepsilon_0}, \tag{4}$$

$$\varepsilon'(\omega) = \frac{K(C_p^{\text{sample}}(\omega) - C_p^{\text{ref}}(\omega) - C_p^{\text{corr}})}{\varepsilon_0}. \tag{5}$$

Due to the imperfect matching of the reference solution small corrections G^{corr} and C_p^{corr} remain. They are read from the data in Figs. 1(c) and 1(d) and taken into account in the subsequent fitting procedure.

B. Complex dielectric function - fit to Cole-Cole expression

In Fig. 2 we show the frequency-dependent imaginary and real part of the dielectric function for the 0.1 mg/mL HA pure water solution. These spectra are calculated according to Eqs. (4) and (5) from the G and C_p spectra [Figs. 1(c) and 1(d)]. The resulting spectra cover the frequency window from 500 Hz to 30 MHz. The reference subtraction procedure has reliably removed the influence of electrode polarization, visible in the raw C_p^{sample} spectra up to 30 kHz, down to 500 Hz. The stray impedance effects noticeable above 10 MHz have shown to be more resilient—the subtraction procedure removed them only up to 30 MHz. We note that the capability of the reference subtraction procedure to remove the EP effects diminishes (low-frequency bound increases) with increasing concentration and total sample conductivity. For this reason the highest successfully analyzed Na-HA concentration was 1.25 mg/mL.

The Cole-Cole function has been widely and successfully used to describe relaxation processes in disordered systems. The dielectric function spectra consist of two broad modes and the data can only be successfully fitted to a sum of two Cole-Cole forms

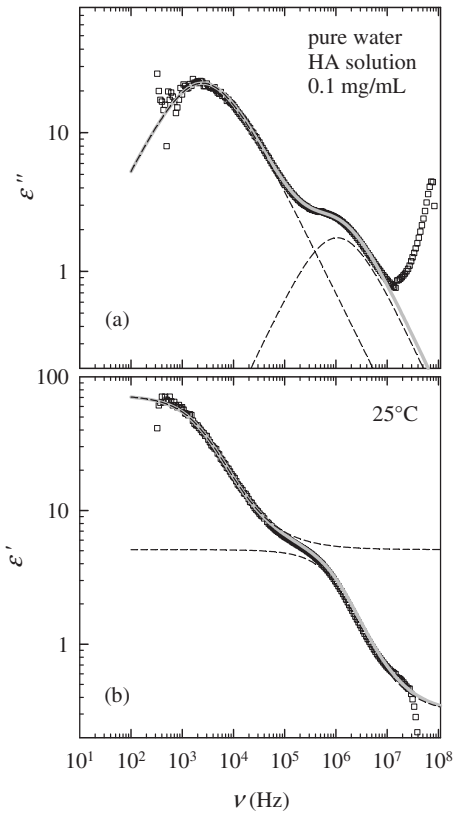

FIG. 2. Double logarithmic plot of the frequency dependence of the imaginary (ε'') and real (ε') part of the dielectric function for the 0.1 mg/mL HA pure water solution. The full lines are fits to the sum of the two Cole-Cole forms (see text); the dashed lines represent a single form.

$$\varepsilon(\omega) - \varepsilon_\infty = \frac{\Delta\varepsilon_{\mathrm{LF}}}{[1 + (i\omega\tau_{0,\mathrm{LF}})^{1-\alpha_{\mathrm{LF}}}]} + \frac{\Delta\varepsilon_{\mathrm{HF}}}{[1 + (i\omega\tau_{0,\mathrm{HF}})^{1-\alpha_{\mathrm{HF}}}]}, \tag{6}$$

where ε_∞ is the high-frequency dielectric constant, $\Delta\varepsilon$ is the dielectric strength, τ_0 the mean relaxation time and $1-\alpha$ the symmetric broadening of the relaxation time distribution function of the LF and HF dielectric mode. Measured data were analyzed by using the least-squares method in the complex plane: the same set of parameters fits both the real and imaginary spectra. Besides improving our ability to resolve two modes, this also provides an important Kramers-Kronig consistency check for the experimental data obtained indirectly by the reference subtraction procedure. This consistency is demonstrated with a Cole-Cole plot (Fig. 3). The larger arch in this figure corresponds to the LF mode, which is more pronounced than the HF one found near the origin of the axes. The final verification of our fits is comparing the $G(\omega)$ data to the conductance spectrum calculated from the dielectric fit parameters using the inverse of the expression 4 [Fig. 1(c), full line].

III. RESULTS

Figure 4 shows the frequency-dependent imaginary and real part of the dielectric function for HA aqueous solutions

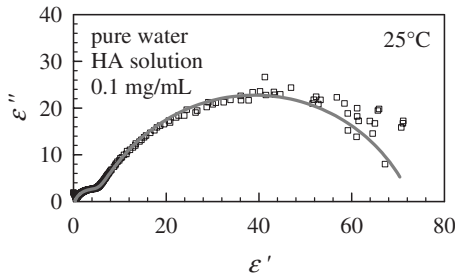

FIG. 3. Cole-Cole plot of the dielectric response for the 0.1 mg/mL HA pure water solution. The full line is a fit to the sum of the two Cole-Cole forms (see text). The LF mode contributes as the dominant arch, while the smaller HF mode is found near the origin of the axes.

with selected HA concentrations. The results for pure water HA solutions (HA concentrations a1=1 mg/mL, a2=0.1 mg/mL, a3=0.0125 mg/mL) are shown in panels (a) and (b), while the results for solutions of 0.03 mg/mL HA concentration with several different added salt concentrations (b1=0 mM, b2=0.12 mM, b3=0.25 mM) are shown in panels (c) and (d). The observed dielectric response is complex and comparable to the one previously observed in DNA solutions. The two broad modes show a symmetrical broadening of the relaxation time distribution function described by the parameter $1-\alpha \approx 0.8$. The mode centered at higher frequencies, $0.15\ \mathrm{MHz} < \nu_{\mathrm{HF}} < 15\ \mathrm{MHz}$, is characterized by dielectric strength $3 < \Delta\varepsilon_{\mathrm{HF}} < 5.5$. The other mode is larger, $20 < \Delta\varepsilon_{\mathrm{LF}} < 150$, and centered at lower frequencies, $0.3\ \mathrm{kHz} < \nu_{\mathrm{LF}} < 50\ \mathrm{kHz}$.

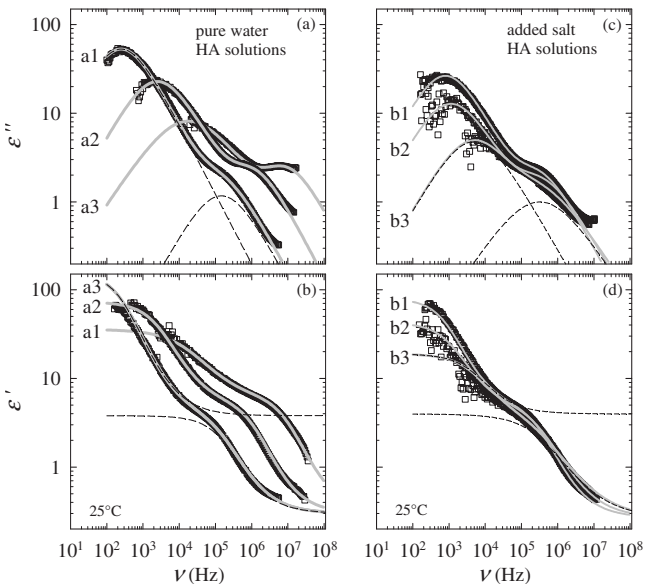

FIG. 4. Double logarithmic plot of the frequency dependence of the imaginary (ε'') and real (ε') part of the dielectric function at $T=25\ ^\circ\mathrm{C}$ of (a), (b) pure water HA solutions for representative a1-a3 (1, 0.1, 0.0125 mg/mL) HA concentrations and (c), (d) HA solutions of concentration $c_{\mathrm{HA}}=0.03$ mg/mL for three representative b1-b3 (0, 0.12, 0.25 mM) added salt concentrations. The full lines are fits to the sum of the two Cole-Cole forms (see text); the dashed lines represent a single form.

The polarization response of polyelectrolyte solutions in the kilohertz to megahertz range is due to oscillations of counterions induced by an applied ac field. Since the counterion displacement happens by diffusion, the dielectric response is basically characterized by the mean relaxation time

$$\tau_0 \propto L^2/D_{\text{in}}. \tag{7}$$

Here L is the associated characteristic length scale, and D_{in} is the diffusion constant of counterions [23]. Experimental data [24] and theoretical estimates [25] show that the renormalization of the diffusion constant of bulk ions due to the presence of polyions is negligible, leading to a value of $D_{\text{in}} = 1.33 \times 10^{-9}$ m^2/s for Na^+ counterions. In other words, the Cole-Cole fits allow us to extract the characteristic time τ_0 and calculate the corresponding length scale for each of the relaxation modes.

While the length scale describes the counterion displacement, the dielectric strength of the relaxation modes is related to the polarizability due to the counterion displacement. The polarizability α is estimated to be proportional to the square of the displacement [4,5], i.e., to the square of the characteristic length scale of the relaxation,

$$\alpha \propto l_B L^2. \tag{8}$$

This scaling form stems from the linear response arguments already invoked by Odijk [26]. Taking into account the number of the relaxing entities, a qualitative expression is reached for the dielectric strength due to the polarizability of the counterion atmosphere around a polyion in polyelectrolytes,

$$\Delta\varepsilon \propto fc\alpha, \tag{9}$$

Combining Eqs. (8) and (9) we get

$$\Delta\varepsilon \propto fcl_B L^2. \tag{10}$$

Here f denotes the fraction of the total counterions of concentration c that take part in a given relaxation. It is important to understand here that the dielectric strength of a mode is primarily defined by the length scale revealed by the mode. The concentration dependence of the fraction of counterions may be deduced by the ratio

$$f \propto \Delta\varepsilon/(cL^2), \tag{11}$$

which is solely based on the experimentally obtained parameters of the dielectric modes.

Similarly complex spectra as shown in Fig. 4 have also been observed for long polydisperse DNA semidilute solutions [6,7]. However, the monomer concentration and added salt dependence measured for HA are rather distinct, indicating that mechanisms of counterion relaxation for HA as compared to long DNA solutions are not identical. Two origins of these differences might be envisaged. First is the rather weak fixed charge on the HA molecule leading to the absence of Manning condensation and second is a much higher flexibility of the HA, whose persistence length is about 9 nm as opposed to 50 nm for the ds-DNA.

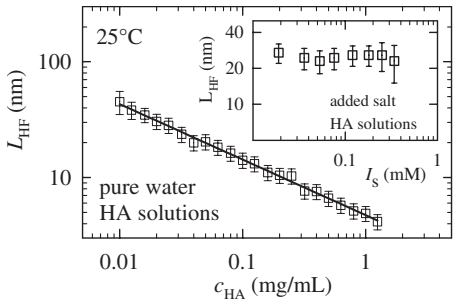

FIG. 5. Main panel: characteristic length of the HF mode (L_{HF}) for pure water HA solutions as a function of HA concentration (c_{HA}). The full line is a fit to the power law $L_{\text{HF}} \propto c_{\text{HA}}^{-0.48\pm0.02}$. Inset: L_{HF} for HA solutions with varying added salt (I_s) for a representative HA concentration $c_{\text{HA}}=0.03$ mg/mL.

A. HF mode

We first describe the characteristics of the HF mode. For pure water HA solutions the characteristic length L_{HF} decreases with increasing HA concentration in two decades wide concentration range following the power law $L_{\text{HF}} \propto c_{\text{HA}}^{-0.48\pm0.02}$ as a function of the HA concentration (main panel of Fig. 5). This dependence -0.48 ± 0.02 suggests that in this regime L_{HF} is proportional to the solution mesh size or the de Gennes-Pfeuty-Dobrynin (dGPD) correlation length ξ that scales as $c_{\text{HA}}^{-0.5}$, as theoretically expected for the salt-free semidilute solutions of flexible polyelectrolytes [4,11,27,28]:

$$\xi \propto f^{-2/7} c^{-1/2}. \tag{12}$$

We note that the fraction of the counterions f, taking part in the relaxation, is here defined by the Manning charge density parameter η as $f=1/\eta=b/l_B$ and is concentration-independent. Therefore, Eq. (12) reduces to $\xi \propto c^{-1/2}$. Finally, we note that the same fundamental length scale is also pertinent for semiflexible chains such as DNA [6,7], as previously predicted by Odijk [26].

A set of data (inset of Fig. 5) for $c_{\text{HA}}=0.03$ mg/mL with varying added salt concentrations shows that the de Gennes-Pfeuty-Dobrynin behavior of L_{HF} remains unchanged at least for all $I_s < 0.34$ mM. Unfortunately for $I_s > 0.34$ mM the accuracy of the data becomes rather unreliable due to progressive merging of the HF and LF modes at these added salt levels making it thus impossible to distinguish the two modes with high enough accuracy. This result nevertheless shows that the dGPD correlation length remains relevant length scale of the HF mode which indeed depends only on the polymer concentration and not on the added salt. It is noteworthy that this holds up to rather high added salt levels as compared to HA counterion concentrations, that is at least up to $2I_s \approx 9c_{\text{in}}$.

The fraction of counterions f_{HF} participating in the HF process is proportional to the normalized dielectric strength $\Delta\varepsilon_{\text{HF}}/(c_{\text{HA}}L_{\text{HF}}^2)$ [see Eq. (11)]. In the main panel of Fig. 6 we show the dependence of $\Delta\varepsilon_{\text{HF}}/(c_{\text{HA}}L_{\text{HF}}^2)$ on HA concentration in pure water solutions. In the inset we show the dependence on the ionic strength of added salt ions for a representative HA concentration $c_{\text{HA}}=0.03$ mg/mL. The data indicate that the fraction of counterions participating in the

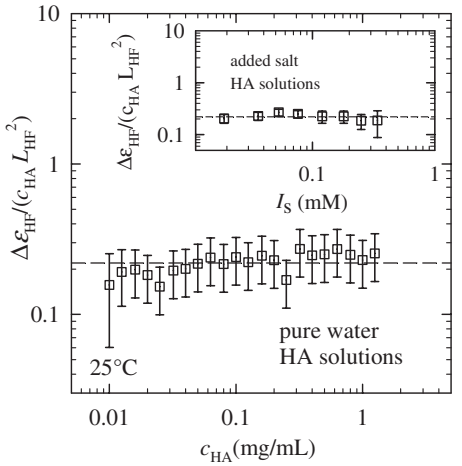

FIG. 6. Main panel: normalized dielectric strength of the HF mode $\Delta\varepsilon_{HF}/(c_{HA}L_{HF}^2)$ as a function of HA concentration c_{HA} for pure water HA solutions. Inset: $\Delta\varepsilon_{HF}/(c_{HA}L_{HF}^2)$ for HA solutions with varying added salt (I_s) for a representative HA concentration $c_{HA}=0.03$ mg/mL. The dashed lines are guides for the eye.

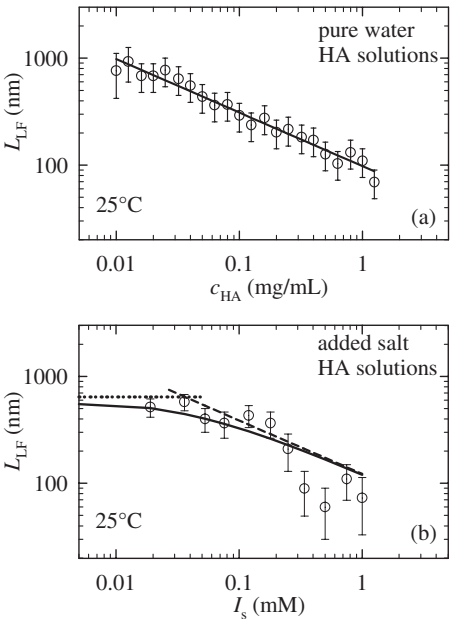

FIG. 7. (a) Characteristic length of the LF mode (L_{LF}) for pure water HA solutions as a function of HA concentration (c_{HA}). The full line is a fit to the power law $r_B=C(B/bc_{HA})^{0.5\pm0.02}$ with $C=4.3$ (see text). (b) L_{LF} for HA solutions with varying added salt (I_s) for a representative HA concentration: $c_{HA}=0.03$ mg/mL. The full line is a fit to the expression $r_{scr}=C\{B/[b(c_{HA}+2AI_s)]\}^{0.5}$ with $C=4.3$ (see text). The dashed line corresponds to $L_p\propto I_s^{0.5}$. The dotted line denotes the value of L_{LF} in salt-free limit for $c_{HA}=0.03$ mg/mL.

HF relaxation process does not depend on the concentration of either HA or added salt in the concentration range studied. Here we point out a similarity with the semidilute DNA solutions where the relaxation mode related to the dGPD correlation length occurs in the same concentration and frequency ranges and features qualitatively similar, concentration-independent f_{HF} [7]. This result validates the standard theoretical models which use the Manning-based definition of f as the concentration-independent parameter. Next, it is worth noting that for DNA f_{HF} remains constant when salt is added to the solution only as long as polyion concentration is substantially larger than I_s. However, as soon as the concentration of added salt ions prevails over the concentration of intrinsic counterions, f_{HF} starts to decrease. Whereas this effect was clearly observed for DNA solutions, in the case of HA it can only be guessed due to smaller accuracy at added salt concentrations larger than 0.2 mM [29].

B. LF mode

We now address the LF mode. For pure water HA solutions, the characteristic length L_{LF} decreases with increasing HA concentration in two decades wide concentration range [Fig. 7(a)] following the power law $L_{LF}\propto c_{HA}^{-0.5\pm0.02}$. This scaling behavior differs from the one observed for long DNA [6,7], where L_{LF} was identified with the average size of the Gaussian chain that behaves as a random walk of correlation blobs and scales as $R\propto c_{DNA}^{-0.25}$ [11,28]. In the case of HA solutions the observed dependence of L_{LF} can be fit nicely to the de Gennes-Dobrynin (dGD) renormalized Debye screening length which scales as

$$r_B = C(B/bc_{HA})^{0.5} \tag{13}$$

in the salt-free regime [28], where we get $C=4.3$. Here the screening is due to HA counterions and the renormalization takes into account the polyion chain properties. r_B has the same scaling as the Debye length, but is larger in magnitude. B is a parameter which is defined as the ratio of the contour length L_c and the actual size L, being close to one for HA, while the monomer size b is 1 nm. Importantly, B is also defined via Manning concentration-independent parameter ($\eta=1/f$) and reads $B=(A^2f)^{2/7}$. A is the average number of monomers between charges. For HA there is no Manning condensation and $A=1$. Now we can write

$$r_B = Cf^{1/7}(bc_{HA})^{-1/2}, \tag{14}$$

which reduces to $r_B\propto c_{HA}^{-1/2}$. Dobrynin *et al.* [28] give only a lower bound of r_B, so that the numerical factor C remains unknown in their calculation. We note that in our previous dielectric spectroscopy experiments [6–8] various length scales correspond to the theoretically expected values not only qualitatively but also quantitatively, i.e., without any rescaling and prefactors [30]. Therefore we take the numerical factor $C=4.3$ as the upper bound up to which the electrostatic screening length expands.

The dependence of L_{LF} on the added salt ionic strength I_s is shown in Fig. 7(b) for $c_{HA}=0.03$ mg/mL. The observed data can be nicely fit to the expression for the electrostatic screening length of the form

$$r_{scr} = C\{B/[b(c_{HA}+2AI_s)]\}^{0.5} \tag{15}$$

with $C=4.3$. Here the electrostatic screening length is almost proportional to the Debye length as first assumed by de Gennes *et al.* [11] and Dobrynin *et al.* [28] for flexible poly-

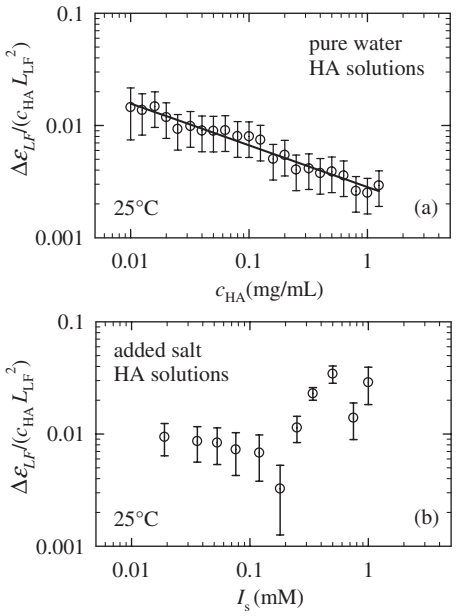

FIG. 8. (a) Normalized dielectric strength of the LF mode $\Delta\varepsilon_{LF}/(c_{HA}L_{LF}^2)$ as a function of HA concentration c_{HA} for pure water HA solutions. The full line is a fit to the power law $\Delta\varepsilon_{LF}/(c_{HA}L_{LF}^2) \propto c_{HA}^{-0.37\pm0.04}$. (b) $\Delta\varepsilon_{LF}/(c_{HA}L_{LF}^2)$ for HA solutions with varying added salt (I_s) for a representative HA concentration $c_{HA}=0.03$ mg/mL.

electrolytes. As before, $B=1$ and $A=1$. We believe that this fit reliably describes the experimental data in spite of poorer accuracy of the data for added salt concentrations close to 1 mM [29]. It is noteworthy that the observed behavior of L_{LF}, that is of the deGennes-Dobrynin (dGD) electrostatic screening length r_{scr}, can be decoupled into high and low salt regimes. In the former, L_{LF} is dominated by the influence of the added salt ions [as shown by dashed line in Fig. 7(b)], whereas the low salt data level off with the limiting value corresponding to the value of L_{LF} found in the salt-free solutions for this HA concentration [see Fig. 7(a)]. This observation indicates how added salt ions and HA counterions compete for the dominant role in the screening of HA polyions revealing at the same time the competition between two length scales describing screening due to two different origins, just as in the case of DNA [6,7]. At vanishing salt L_{LF} can be identified as the renormalized Debye screening length due to HA counterions only $r_B=C(B/bc_{HA})^{0.5}$, while, by analogy with DNA, for finite added salt L_{LF} can be identified as the electrostatic persistence length that apparently depends linearly on the Debye length and can be fitted to the form $L_p \propto I_s^{-0.5}$. It is noteworthy that the power law which thus describes the electrostatic persistence length for HA differs from the one found for long DNA chains [6,7], which corresponds to the Odijk-Skolnick-Fixman (OSF) electrostatic persistence length scaling as $L_p \propto I_s^{-1}$ [31,32].

The normalized LF mode dielectric strength $\Delta\varepsilon_{LF}/(c_{HA}L_{LF}^2)$ is shown in Fig. 8: panel (a) displays its dependence on HA concentration in pure water solutions, and panel (b) dependence on the ionic strength of added salt ions for a representative HA concentration $c_{HA}=0.03$ mg/mL. Again we assume that the dielectric strength was defined by the square of the length scale revealed by a given relaxation, and also by the concentration of the relaxation entities, i.e., fraction of counterions f_{LF} participating in the LF relaxation [see Eq. (10)]. In this manner the normalized dielectric strength presented in the panel (a) shows that the apparent fraction of counterions participating in the LF relaxation strongly decreases with an increase in HA concentration according to a power law $f_{LF} \propto \Delta\varepsilon_{LF}/(c_{HA}L_{LF}^2) \propto c_{HA}^{-0.37\pm0.04}$. This reflects the decrease in the dielectric strength $\Delta\varepsilon_{LF}$ of the mode itself, since the product $(c_{HA}L_{LF}^2)$ is a constant due to the fact that L_{LF} is a renormalized Debye screening length which scales as $c_{HA}^{-0.5}$ [see Eq. (14)]. This result indicates that the concentration-independent Manning-based definition for the number of oscillating counterions is not valid in this case. Presumably, as the screening due to other polyions and counterions increases with concentration it might reduce the effective number of counterions participating in the LF relaxation along the renormalized Debye length r_B. On the other hand, data displayed in panel (b) suggest that f_{LF} becomes larger in the case of added salt solutions compared to the pure water case, once the concentration of added salt ions becomes larger than c_{HA} and relaxation happens along the electrostatic persistence length. A similar effect was observed for DNA solutions and ascribed to the intrinsic counterion atmospheres squeezed closer to the chains [7].

IV. DISCUSSION

First, we comment the issue of respective roles in screening of HA counterions and ions from the added salt in the light of previously obtained results on long DNA [6,7]. For both systems the influence of added salt is important as long as the added salt concentration $2I_s$ is sufficiently larger than the concentration of intrinsic counterions c_{in}. However, whereas for DNA we observed that these two regimes are delimited at about $2I_s/c_{in} \approx 0.4$, for Na-Ha this occurs at higher added salt levels $2I_s/c_{in} \approx 1$. Since in the case of HA all intrinsic counterions are free, while there are only 25% free in the case of DNA, this result might indicate that the effective counterion screening is due primarily to the free counterions and not to condensed ones. Such a result is not surprising since the proper description of strongly charged polyelectrolytes such as DNA, with large charge densities that produce nonlinearities, is standardly tackled by taking into account the Manning condensation while retaining the linearized Debye-Hückel (DH) theory for the remaining salt. Conversely, in the case of weakly charged polyelectrolytes, such as HA, the DH approximation can be used without fundamental modifications.

Second, our understanding of the LF mode provides additional details in the scenario for the HF mode. We remind that in the case of the long DNA the dGPD correlation length gives way to the Debye screening length as a new relevant length scale for HF mode. This occurs exactly when sufficient salt is added so that the corresponding Debye screening length becomes comparable to and eventually smaller than the dGPD correlation length [7]. On the other hand, in the case of HA the screening length is revealed as the pertinent length scale for the LF mode. Only at very high added salt

concentrations, the screening length and the correlation length observed in the HF mode, will theoretically become comparable. For example, at $c_{HA}=0.03$ mg/ml the correlation length $L_{HF}\approx 25$ nm (see Fig. 5) could become comparable to L_{LF} at added salt concentration $I_s\approx 30$ mM [see Fig. 7(b)]. Thus we expect the correlation length to remain relevant for HF mode at the added salt concentrations at least one order of magnitude higher than practically measurable with our technique.

In what follows we address possible reasons for why the LF relaxation mode observed for the HA polyelectrolyte yields L_{LF} scaling laws which differ from the ones observed in the long DNA case [6,7]. The first issue concerns the salt-free regime in which the average size of the Gaussian chain which scales as $c^{-0.25}$, previously observed for long DNA, is replaced in the case of HA by the renormalized Debye screening length which scales as $r_B=C(B/bc_{HA})^{0.5}$. We suggest that the absence of Manning condensed counterions due to weaker electrostatic interactions, characterized by a charge density parameter $\eta<1$, might be at the origin of this observation. We base this suggestion on the experimental data on long DNA, reported before, that have indicated that for the LF relaxation in the salt-free regime it is mostly the condensed counterions that oscillate along or in close proximity to an individual chain in the polyelectrolyte solution, except at large enough salt concentrations where at least some of the free counterions seem to join in playing this role. Contrary, in the case of HA only free counterions, Manning condensed being absent, participate in the LF relaxation and their oscillation in the volume around the chain naturally brings in the renormalized Debye screening length, which has a stronger concentration dependence and therefore appears as a more pertinent length scale than the average size of the chain.

The second issue is why for HA with finite added salt the characteristic length scale of counterion dynamics, that for DNA allowed an association with the OSF electrostatic persistence length, is replaced by the electrostatic persistence length which scales linearly with Debye length κ^{-1}, i.e., as $L_p\propto I_s^{-0.5}$. We consider it plausible that a much higher flexibility of HA, as compared to DNA, might be responsible for this change, so that the OSF approach in which the chain is modeled as a rigid rod would be invalidated. This has been already stressed and discussed at length by Ullner [33,34] and others [35,36]. Here we note that the controversy concerning the conformational properties of flexible polyelectrolytes in the presence of added salt has been discussed over the last fifty years without reaching a firm consensus [33]. In particular, the electrostatic persistence length has been reported to depend both quadratically and linearly on the Debye screening length. The former is a result of the analytical approaches based on the OSF-like perturbational calculation in which the polyelectrolyte is modeled as a rigid rod, whereas the latter comes out from the variational calculation for a Flory-type flexible chain. A weak point in both approaches is the assumption that there is a single behavior that describes the chain on all length scales. Recently, Ullner has argued [34] that a consistent picture might emerge taking into account simulations with a careful analysis of analytical approaches. According to his arguments, three regimes can be distinguished with respect to the scaling of the persistence length with the Debye screening length. In the first two regimes where κ^{-1} is larger or comparable to the size of the chain, R, the chain thus being rather stiff, it behaves as a rodlike chain, so that the OSF approach is valid and $L_p\propto I_s^{-1}$. In the third regime where κ^{-1} is small or the chain is weakly charged [36], the chain is flexible enough to allow distant parts to get close, which gives rise to increased long-range correlations so that the excluded volume effects start playing an important role which affects the average size of the molecule in a way that corresponds to a linear or even a sublinear dependence of the persistence length on the ionic strength I_s. There are various expressions for the scaling exponent of the electrostatic persistence length on the ionic strength in this regime, with the simplest one yielding behavior close to $I_s^{-0.5}$ [33–36].

Obviously these excluded volume effects are much less pronounced in the case of DNA, which is intrinsically a stiff molecule. We find it difficult to apply the criterion κ^{-1} versus the chain size R in the case of experimentally studied system, since κ^{-1} is always much smaller than R. Rather we suggest that the comparison of the structural persistence length L_0 and the correlation length ξ should be more meaningful in this regard. Indeed, the comparison of L_0 (50 nm for DNA and 9 nm for HA) and the correlation length ξ in the same concentration range (10–50 nm for DNA and 4–45 nm for HA) indicates that while for DNA $L_0\geq\xi$, for HA exactly the opposite relationship holds, $L_0\leq\xi$, indicating a much higher HA flexibility if compared to DNA. This stronger flexibility of HA leads in its turn to a weaker dependence of the electrostatic persistence length on added salt concentration because of the more pronounced excluded volume effects. Indeed, by reanalyzing viscosity data Tricot has demonstrated the validity of $L_p\propto I_s^{-0.5}$ for different flexible polyelectrolytes with structural persistence length between 2 and 20 nm [37]. In addition, he has shown that L_p does not diverge at vanishing added salt concentration, rather it reaches the maximum value that may be much smaller than the polymer extended length L. Additional confirmation to corroborate these results comes from transient electric birifrigence measurements performed on flexible Na-PSS for a range of low added salt concentrations similar to ones used in our dielectric spectroscopy measurements [38].

On the other hand, recent small angle neutron scattering (SANS) experiments on HA for added salt concentrations larger than 1 mM, reveal the OSF behavior for the electrostatic persistence length [10,39]. However, a closer inspection of Fig. 10 in Ref. [10] and of Fig. 3 in Ref. [39] reveals that the apparent OSF behavior of data critically depends on the 0.1 M (0.2 M) single data point which is not obtained from experiment, but is rather calculated from the OSF formula. This result apparently contradicts our results obtained by dielectric spectroscopy measurements, but only for added salt concentrations smaller than 1 mM. We can conceive two possible reasons for this discrepancy. The first cause might be associated with different added salt regimes. Another cause might lie in the fact that the SANS experiments were done on much shorter HA chains than our DS experiments, and the analysis of the SANS data was based on theory in which excluded volume effects were neglected. In future,

more efforts are needed in order to elucidate the crossover behavior between low and high added salt regimes as far as HA and other flexible polyelectrolytes are concerned. This task however appears to be a rather difficult one for the following reason. The low added salt regime, below a few mM, can be probed only by very few experimental techniques, which cannot be used for high added salt concentrations, among which dielectric spectroscopy appears as the most reliable one. The opposite holds for the high salt regime above 5 mM or so: a number of techniques, while they cannot be used for low added salt, can cover this regime ranging from viscosity measurements to SANS experiments. It thus seems impossible to find a single technique for continuously following the conformational change of the polyion over a broad added salt concentration range.

All these results make it quite clear that the standard criterion to discriminate flexible against semiflexible polyelectrolytes, which compares the structural persistence length with the monomer size, cannot be always strictly applied. It also appears difficult to apply the criterion κ^{-1} *vs.* R as argued by Ullner *et al.* [34]. Another criterion which considers the structural persistence length in comparison with the correlation length appears to be of key importance which determines, at least for added salt concentrations below few mM, the outcome of two competing electrostatic persistence lengths: the one scaling linearly with the Debye length versus the one scaling quadratically with the Debye length, i.e., the Odijk-Skolnick-Fixman length. Keeping this in mind, regarding the salt dependence of its persistence length the HA seems to be somewhere in between the semiflexible DNA and the flexible Na-PSS.

V. CONCLUSION

In conclusion, our results demonstrate that in the case of low added salt there are basically two fundamental length scales that determine the dielectric response of semidilute solutions of semiflexible polyelectrolyte HA: de Gennes-Pfeuty-Dobrynin semidilute solution correlation length and de Gennes-Dobrynin electrostatic screening length. The first length scale is important for the high-frequency response, while the second one is important for the low-frequency response. Collective properties probed by the high-frequency dielectric relaxation are thus well described by the de Gennes-Pfeuty-Dobrynin solution correlation length predicted and proven to be valid for both flexible and semiflexible chains. Single-chain properties probed by the low frequency relaxation are described by the electrostatic persistence length that scales linearly with the Debye length, contrary to the DNA case where the scaling is quadratic as rationalized by the OSF formula. This difference is most probably due to the fact that the HA chain is much more flexible than the DNA chain, precluding the straightforward application of the OSF arguments. This also indicates that HA, as far as its flexibility is concerned, is half-way between semiflexible and completely flexible polyelectrolytes. In the salt-free regime the de Gennes-Dobrynin screening length is due to HA counterions only, which can thus be described by a renormalized Debye screening length that apparently prevails as the fundamental single-chain property probably due to the absence of the condensed counterions in the weakly charged polyelectrolyte. Finally, our results reveal that the standard theoretical approaches based on the concentration-independent Manning parameter η face some limitations when applied to the dielectric response of the counterion atmosphere around polyions. These theories describe well the HF dielectric relaxation along the correlation length, with its concentration-independent fraction of oscillating counterions $f=1/\eta$. On the other hand, they fail to offer a proper description of the LF relaxation characterized by the renormalized Debye screening length. For this relaxation, the effective number of counterions decreases with increasing concentration, which might be ascribed to enhanced screening due to other polyions and counterions.

ACKNOWLEDGMENTS

We would like to thank P. A. Pincus for a valuable and illuminating discussion. This work was supported by the Croatian Ministry of Science, Education and Sports under Grant No. 035-0000000-2836 (Strongly correlated inorganic, organic and biomaterials). R.P. would like to acknowledge the financial support by the Slovenian Research Agency under Contracts No. P1-0055 (Biophysics of Polymers, Membranes, Gels, Colloids and Cells) and No. J1-0908 (Active media nanoactuators with dispersion forces). This study was in part supported by the Intramural Research Program of the NIH, Eunice Kennedy Shriver National Institute of Child Health and Human Development.

[1] M. Daune, *Molecular Biophysics* (Oxford University Press, New York, 2003).
[2] V. A. Bloomfield, D. M. Crothers, and I. Tinocco, Jr., *Nucleic Acids* (University Science Books, Sausalito, 2000).
[3] H. G. Elias, *Macromolecules* (Plenum Press, New York, 1984).
[4] F. Bordi, C. Cametti, and R. H. Colby, J. Phys.: Condens. Matter **16**, R1423 (2004).
[5] K. Ito, A. Yagi, N. Ookubo, and R. Hayakawa, Macromolecules **23**, 857 (1990).
[6] S. Tomić, T. Vuletić, S. Dolanski Babić, S. Krča, D. Ivanković, L. Griparić, and R. Podgornik, Phys. Rev. Lett. **97**, 098303 (2006).
[7] S. Tomić, S. Dolanski Babić, T. Vuletić, S. Krča, D. Ivanković, L. Griparić, and R. Podgornik, Phys. Rev. E **75**, 021905 (2007).
[8] S. Tomić, S. Dolanski Babić, T. Ivek, T. Vuletić, S. Krča, F. Livolant, and R. Podgornik, EPL **81**, 68003 (2008).
[9] N. Nandi, K. Bhattacharyya, and B. Bagchi, Chem. Rev. (Washington, D.C.) **100**, 2013 (2000).
[10] E. Buhler and F. Boue, Macromolecules **37**, 1600 (2004).

[11] P. G. De Gennes, P. Pincus, R. M. Velasco, and F. Brochard, J. Phys. (Paris) **37**, 1461 (1976).
[12] c^* is given by the concentration where there is only one polymer molecule in the volume of a polymer globule c^* = molecule mass/V_c, where molecule mass is $N \cdot m_m$, and $V_c \approx L_c^3 = N^3 \cdot b^3$; m_m is a mass of a monomer ≈401 g/mol, N = 4000, $L_c = N \cdot b$; b = 1 nm; b is the monomer size.
[13] H. P. Schwan, G. Schwarz, J. Maczuk, and H. Pauly, J. Phys. Chem. **66**, 2626 (1962).
[14] C. G. Essex, G. P. South, R. J. Sheppard, and E. H. Grant, J. Phys. E **8**, 385 (1975).
[15] H. Haruta, *The Impedance Measurement Handbook*, 2nd ed. (Agilent Technologies Inc., Santa Clara, CA, 2000).
[16] A. D. Hollingsworth and D. A. Saville, J. Colloid Interface Sci. **257**, 65 (2003).
[17] R. Roldán-Toro and J. D. Sollier, J. Colloid Interface Sci. **274**, 76 (2004).
[18] H. P. Schwan and C. D. Ferris, Rev. Sci. Instrum. **39**, 481 (1968).
[19] C. L. Davey, G. H. Markx, and D. B. Kell, Eur. Biophys. J. **18**, 255 (1990).
[20] B. Saif, R. K. Mohr, C. J. Montrose, and T. A. Litovitz, Biopolymers **31**, 1171 (1991).
[21] C. Grosse, M. Tirado, W. Pieper, and R. Pottel, J. Colloid Interface Sci. **205**, 26 (1998).
[22] F. Oosawa, *Polyelectrolytes* (Marcel Dekker, New York, 1971).
[23] R. W. O'Brian, J. Colloid Interface Sci. **113**, 81 (1986).
[24] T. E. Angelini, R. Golestanian, R. H. Coridan, J. C. Butler, A. Beraud, M. Krisch, H. Sinn, K. S. Schweizer, and G. C. L. Wong, Proc. Natl. Acad. Sci. U.S.A. **103**, 7962 (2006).
[25] F. Bordi, C. Cametti, and T. Gili, Phys. Rev. E **66**, 021803 (2002).
[26] T. Odijk, Macromolecules **12**, 688 (1979).
[27] P. Pfeuty, J. Phys. (Paris) **39**, C2-149 (1978).
[28] A. V. Dobrynin and M. Rubinstein, Prog. Polym. Sci. **30**, 1049 (2005); A. V. Dobrynin, R. H. Colby, and M. Rubinstein, Macromolecules **28**, 1859 (1995).
[29] The lower accuracy of our data for added salt concentrations above 0.2 mM are due to strong influence of the electrode polarization effects.
[30] Data obtained on the long and short 146 bp DNA fragments give 50 nm value for the structural persistence length and 50 nm value for the contour length, respectively.
[31] T. Odijk, J. Polym. Sci., Polym. Phys. Ed. **15**, 477 (1977).
[32] J. Skolnick and M. Fixman, Macromolecules **10**, 944 (1977).
[33] M. Ullner, in *DNA Interactions with Polymers and Surfactants*, edited by R. Dias and B. Lindman (Wiley-Interscience, New York, 2008).
[34] M. Ullner, J. Phys. Chem. B **107**, 8097 (2003).
[35] J. L. Barrat and J. F. Joanny, EPL **24**, 333 (1993).
[36] A. V. Dobrynin, Macromolecules **38**, 9304 (2005).
[37] M. Tricot, Macromolecules **17**, 1698 (1984).
[38] V. Degiorgio, F. Mantegazza, and R. Piazza, EPL **15**, 75 (1991).
[39] F. Bonnet, R. Schweins, and F. Boue, EPL **83**, 48002 (2008).